Check for updates

FEBS Letters

FEBS PRESS science publishing by scientists

EDITOR'S CHOICE

Structural considerations of folded protein import through the chloroplast TOC/TIC translocons

Iniyan Ganesan and Steven M. Theg

Department of Plant Biology, University of California Davis, CA, USA

Correspondence
S. M. Theg, Department of Plant Biology, University of California Davis, One Shields Avenue, Davis, CA 95616, USA
Tel: 530-752-0624
E-mail: smtheg@ucdavis.edu

(Received 9 January 2019, revised 13 February 2019, accepted 15 February 2019, available online 5 March 2019)

doi:10.1002/1873-3468.13342

Edited by Julian Schroeder

Protein import into chloroplasts is carried out by the protein translocons at the outer and inner envelope membranes (TOC and TIC). Detailed structures for these translocons are lacking, with only a low-resolution TOC complex structure available. Recently, we showed that the TOC/TIC translocons can import folded proteins, a rather unique feat for a coupled double membrane system. We also determined the maximum functional TOC/TIC pore size to be 30–35 Å. Here, we discuss how such large pores could form and compare the structural dynamics of the pore-forming Toc75 subunit to its bacterial/mitochondrial Omp85 family homologs. We put forward structural models that can be empirically tested and also briefly review the pore dynamics of other protein translocons with known structures.

Keywords: BamA; chloroplast protein import; Sam50; TIC; TOC

Protein import into chloroplasts, an essential process for plant development and photosynthesis, is carried out by the protein translocons at the outer and inner envelope membranes (TOC and TIC). The TOC complex components have long been identified and low-resolution structural information is available [1]. However, structural information for the TIC complex is lacking, aside from a few soluble domain structures. More pressingly, the protein composition of the TIC complex and the TIC pore is still under debate [2–4]. Recently, we showed that proteins as large as 22 kDa can be imported into chloroplasts in a folded conformation and that the maximum TOC/TIC pore size is significantly larger than previously thought [5]. Here, we discuss how such large TOC/TIC pores may form and briefly review the pore dynamics of other protein translocons with known structures.

Located in the TOC complex are the subunits Toc75, Toc34, and Toc159. The major pore-forming subunit is Toc75, a 16-stranded β-barrel homolog of bacterial BamA and mitochondrial Sam50. Toc159 has also been proposed to form part of the pore because its membrane domain crosslinks to import-intermediate substrates [6]. This 52-kDa membrane domain is resistant to thermolysin and trypsin treatment [7,8] and, therefore, likely contains multiple membrane spanning regions, the structure or even topology of which are unknown. Toc75, Toc34, and Toc159 are complexed in a 4 : 4 : 1 ratio as determined by multiple methods; a low-resolution structure suggests a complex containing four pores [1]. A 3 : 3 : 1 ratio has also been proposed based on immunoblot quantification of TOC subunits from total chloroplast samples relative to purified samples [9]; however, antibody reactivity can sometimes be variable between purified antigens and antigens within complex mixtures such as those derived from total chloroplasts.

As the major pore-forming subunit in the inner membrane, Tic20 is part of both proposed TIC complexes, the Tic110 and 1-MDa complexes [4]. The 1-MDa complex contains Tic20, Tic55, Tic100, and Tic214, all of which are proposed to exist in equimolar ratios in a trimeric complex. [10]. The Tic110 complex migrates at ~230 kDa on BN-PAGE, but the

Abbreviations
DHFR, dihydrofolate reductase; MTX, methotrexate; TMHs, transmembrane helices.

stoichiometry of this complex has not been determined [10,11]. Tic110, which does not associate with the 1-MDa complex, has been proposed to function as a scaffold for stromal chaperones [12–14]. Tic110 has also been proposed to function as the pore itself [2]. However, unlike Tic20, Tic110 has not been consistently crosslinked to import-intermediate substrates and channel formation depends on a membrane topology that is disputed [2,3,15].

Structural considerations of a large TOC complex pore

Structures solved at high resolution for the membrane domains of the TOC components are not currently available. However, the Toc75 structure can be inferred by homology modeling with the known structure of BamA [16] (Fig. 1A). A pore cross section of the space-filled Toc75 structure is roughly circular and has a pore diameter of ~20 Å. Currently, there is no direct evidence that substrates pass through the Toc75 central channel, but this is likely for the following reasons: (a) Substrates pass through the central channel of the well-characterized β-barrel proteins Tom40 and FhaC [17,18]. FhaC and Toc75 are both members of the same Omp85 superfamily. (b) Substrates of Sam50 enter its central channel before being integrated into the membrane [19]. (c) Inward facing residues of the Toc75 barrel tend to be more hydrophilic than outward facing resides. Internal and external residues have a GRAVY score of −1.1 and 0.7, respectively. The GRAVY score is the average Kyte and Doolittle sidechain hydrophobicity value per residue [20]. Since the translocation path traverses the central Toc75 channel and the maximum pore diameter of TOC/TIC is larger than this single Toc75 channel, we expect the Toc75 barrel to open and generate a larger pore. There is reason to believe this is possible since the terminal β-strands of Toc75 are structurally similar to the BamA/Sam50 homologs, which have weakly interacting terminal β-strands [4]. Recently, the mechanism of β-barrel insertion via Sam50 was described wherein the first and last β-strands of Sam50 pair with incoming substrate β-strands [19]. Once the substrate β-barrel protein is fully inserted in the membrane, its terminal β-strands would be paired with the terminal β-strands of Sam50. Finally, the substrate β-barrel structure closes and buds off from Sam50. Most intriguingly, BamA has been proposed to form a transient large pore in conjunction with one of its β-barrel autotransporter substrates, EspP [21]. Autotransporters have a C-terminal β-barrel domain that integrates into the outer membrane and exports an N-terminal soluble

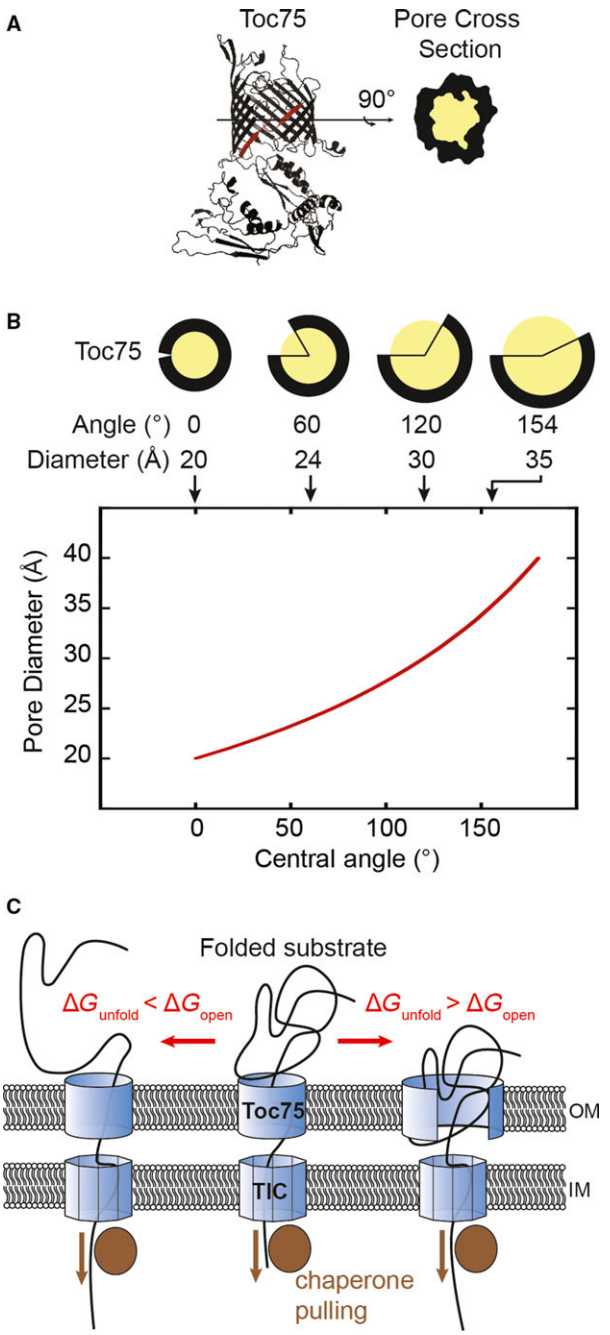


Fig. 1. Toc75 barrel opening. (A) The structure of *Pisum sativum* Toc75 was obtained by threading the sequence with Phyre2 [54]. The first and last β-strands are highlighted in red. The roughly circular Toc75 barrel (black) and pore (yellow) are shown as a cross section in the membrane plane. (B) The circular pore diameter obtained from open conformations of Toc75 is plotted as a function of the Toc75 central opening angle. (C) Toc75 barrel opening is likely driven by the pulling force exerted on folded substrates by stromal chaperones. Under this model, the barrel would only open if the energetics of barrel opening (ΔG_{open}) is more favorable than substrate unfolding (ΔG_{unfold}).

passenger domain. The EspP passenger domain is known to fold in the periplasm to an extent that it is too large to pass through the 10 Å diameter pore of EspP. Analysis of EspP targeting suggests that during β-barrel membrane insertion via BamA, the EspP barrel generates a combined pore with the BamA barrel through which the EspP passenger domain is exported [21]. These processes would require the Sam50/BamA barrels to be quite flexible, allowing for the hypothesis that Toc75 could be flexible as well.

The maximum TOC/TIC pore size is 30–35 Å [5], and thus the Toc75 barrel would need to open to a maximum angle of 120–154°, as measured from the pore center (Fig. 1B). This is a rather large conformational change; however, we do not expect the Toc75 barrel to freely open to this maximum pore size. For example, if the maximum pore size were 31 Å, the import efficiency of a 30 Å fixed-diameter substrate would be nearly zero. Indeed, we observed an inverse relationship between substrate size and import efficiency in the 13–28 Å range [5]. We might expect the Toc75 barrel to only open/expand if the energy required for barrel opening/expansion is lower than the energy required to unfold a substrate (Fig. 1C). Both barrel opening/expansion and unfolding of stable substrates may very well be driven by the same energy source: stromal ATPase chaperones. These roles for stromal chaperones are supported by the observations that ~80 residues of N-terminal unstructured sequence (to span both membranes) is required for efficient import of a stably folded substrate and that the transit peptide N terminus is exposed to the stroma before the final energetic import step requiring high concentrations (>1 mM) of ATP [22,23].

In light of the TOC complex stoichiometry and since Toc159 can only insert into membranes containing the other TOC components [24], Toc159 is likely located in the center of the complex surrounded by four Toc75 subunits (Fig. 2). In this model, cross sections of Toc75 and Toc159 are depicted within the plane of the membrane; Toc34 is not shown, as it has not been implicated in pore formation. As the Toc75 barrel opens, the open portion of the pore must be filled in by other TOC components, potentially other Toc75 subunits and/or Toc159 (Fig. 2). It seems intuitive that the terminal β-strands of Toc75 could pair with neighboring Toc75 subunits since BamA/Sam50 terminal β-strands pair with other β-barrel substrates. In fact, the neighboring Toc75 β-strands may already be paired in the resting state of the TOC complex (Fig. 2, Open Resting State) since the four pores found in the low-resolution TOC structure (presumably corresponding to four Toc75 channels) seem to be connected [1]. Alternatively, the Toc75 barrels could be closed in the resting state (Fig. 2, Closed Resting State). From these resting states, expanded pores actively importing stably folded proteins could potentially arise in many configurations involving Toc159 and/or additional Toc75 subunits as illustrated. The expanded pores are depicted with the maximum pore diameter of 35 Å to clearly illustrate pore expansion. Again, it should be cautioned that we do not expect the Toc75 barrel to readily open to this fully expanded state and the maximum pore size may only be 30 Å. Also, these models are suggestions of the most likely scenarios given what is currently known, rather than a complete accounting of all possibilities.

Determining the veracity of these TOC complex pore models will require further investigation. An

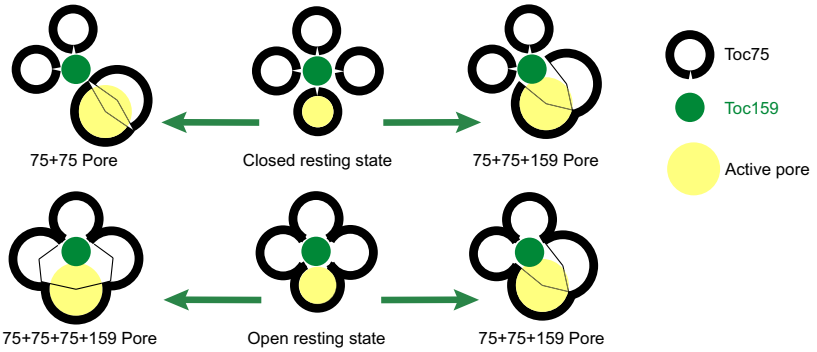


Fig. 2. Models for TOC complex pore expansion to accommodate folded proteins. Toc75 and Toc159 are shown as cross sections in the membrane plane. Various models show TOC pore expansion involving the Toc75 barrel opening along with combinations of other Toc75 subunits and Toc159 sealing the remainder of the open pore perimeter. It should be noted that Toc159 is not necessarily drawn to scale relative to Toc75 since the structure/topology of the Toc159 membrane domain is unclear. Toc34 is not shown.

illuminating line of experimentation to better understand the role of Toc75 barrel opening would be based on locking the barrel into a closed structure by generating intramolecular disulfide bonds between the terminal β-strands of Toc75. Locking the lateral gate of BamA has been shown to impair function *in vivo* and *in vitro* [25,26]. Locking the Toc75 barrel is theoretically possible in Arabidopsis through complementation of Toc75 mutants [27,28]. Crosslinking the Toc75 terminal β-strands could determine whether Toc75 is closed or open in the resting state (Fig. 2) based on whether multiple Toc75 subunits crosslink under oxidizing conditions. It would be of great interest to determine the import efficiencies of folded and unfolded substrates (i.e., DHFR with or without MTX) across crosslinked and non-crosslinked Toc75 complexes. We would expect locking the Toc75 barrel closed to have a greater effect on folded protein import than unfolded protein import, although it may potentially block the import of both.

Parallel to the barrel locking experiment, single cysteine Toc75 mutants could be generated to analyze site-specific crosslinks from the Toc75 barrel to other TOC subunits. This could help map out how the Toc75 subunits are arranged in relation to Toc159. Toc75 contains many native cysteines and two of those located in the POTRA domains have been proposed to form a potentially important disulfide bridge [29]. If these POTRA cysteines cannot be substituted, Toc75 β-barrel crosslinks could be specifically analyzed after removing the POTRA domains by trypsin treatment.

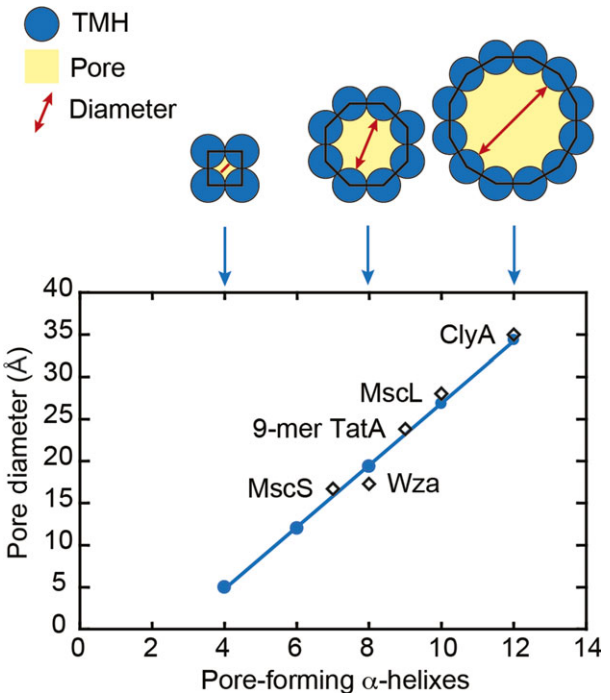


Fig. 3. Number of TIC complex pore-forming helices required to accommodate folded proteins. Assuming an average helix diameter of 12 Å and a regular polygonal arrangement of the helices, the pore diameter is plotted as a function of the TMH number required to form such a pore (blue line). As validation, values for relatively large α-helical pores of known structure were plotted as well (black diamonds). These structures include the open conformations of the mechanosensitive channels, MscS and MscL [38,55,56], the bacterial outer membrane polysaccharide export channel, Wza [57], the pore-forming toxin, ClyA [58], and a modeled structure of a TatA 9-mer [59].

Structural considerations of a large TIC complex pore

Other than the rather trivial fact that the TIC subunits are composed of α-helical transmembrane proteins, there is no structural information regarding the TIC complex pore. However, given the maximum pore size measured for TOC/TIC (30–35 Å), the average α-helix diameter (12 Å), and assuming the pore-forming transmembrane helices (TMHs) are arranged in a regular polygonal shape in the membrane plane, we can at least estimate the number of helices required to produce such a large pore. Under these assumptions, there is a linear relationship between pore size and pore-forming TMHs (Fig. 3, blue line). It would require at least 11–12 TMHs to generate a 30–35 Å pore. As a proof of concept, the pore diameters of relatively large α-helical pores of known structure are also plotted as a function of pore-forming helix number (Fig. 3, black diamonds).

Recognizing that the 1-MDa TIC complex contains three copies of Tic20 [10], a 12 TMH pore could theoretically be generated within the 1-MDa complex if all four TMHs of Tic20 are pore-forming. It is unclear how many Tic20 subunits are involved in the Tic110 complex model. A Tic110 pore is predicted to be formed by a total of eight TMHs derived from two Tic110 subunits [2]. It is unclear where the additional 3–4 TMHs would come from to generate the 11–12 TMH expanded pore. The Tic110 complex migrates at ~230 kDa, so it seems unlikely to contain more than two Tic110 subunits. The other components of the Tic110 complex seem unlikely to contribute to pore formation since Tic40 contains only one very hydrophobic TMH and the other Tic110 complex components play regulatory roles [2]. The maximum TOC/TIC pore size seems to be more consistent with a 1-MDa TIC complex pore rather than a Tic110 pore, although multiple TIC complexes with variable

maximum pore sizes could exist in the inner membrane. However, it should be noted that Tic110 has already become somewhat disfavored as the pore-forming TIC component, as reviewed elsewhere [3,4].

Experiments utilizing a crosslinking approach similar to that described for Toc75 could map out the positioning of subunits within the TIC complex. Single cysteine Tic20 mutants can be generated to analyze site-specific crosslinks between Tic20 and other TIC components or substrates. For example, it would be interesting to see whether the three Tic20 subunits are located in close proximity within the 1-MD complex. Crosslinks between Tic20 TMH cysteines and substrates could determine which TMHs participate in pore formation. A fluorescence approach measuring substrate-dependent changes to pore hydrophobicity, similar to a Tim23 study [30], could also be attempted.

Mechanistic considerations of folded protein import for stromal chaperones

Several chaperones have been implicated in generating the driving force for protein import into chloroplasts. In chronological order, these chaperones include Hsp93, Hsp70, Hsp90, and recently Ycf2/FtsHi [31–33]. The chaperones act on the unstructured N-terminal transit peptide of the substrate, so the foldedness of the substrate mature domain does not radically affect our thinking on how these chaperones function. In other words, by the time the stromal chaperone encounters a folded mature domain, the folded mature domain would already be at least halfway across the inner membrane.

Roles for chaperones as translocation motors have been classified by Brownian ratchet, power stroke, or entropic pulling mechanisms [34]. It was recently suggested that the Ycf2/FtsHi complex may be responsible for the ability of chloroplasts to import folded proteins in contrast to mitochondria, which utilize mtHsp70 and $\Delta\psi$ to drive import of unfolded substrates [35]. It was further suggested that the power stroke mechanism of Ycf2/FtsHi would generate more pulling force than the Brownian ratchet mechanism of Hsp70. However, the generation of force by Hsp70 is actually better characterized by the entropic pulling model, which combines properties of the power stroke and Brownian ratchet mechanisms [36,37]. Entropic pulling is predicted to generate forces comparable to the power stroke [36], but it is not entirely clear how entropic pulling (or power stroke) would be affected by a folded substrate. Therefore, it is currently unclear which chaperones, if any, are better suited to handle folded substrates. Regardless of the chaperone pulling force issue, the identity of the import motor(s) does not necessarily illuminate the discussion of the ability to import folded proteins. Rather, the contrast between the capabilities of chloroplast and mitochondrial import machineries likely stems from differential flexibility of their respective pore-forming components.

Despite extensive study, a major experimental difficulty seems to be assigning the role of stromal chaperones as genuine import motors or as downstream quality control and substrate refolding factors [3,4]. Since chloroplasts can import dihydrofolate reductase (DHFR) complexed with methotrexate (MTX) in a folded conformation [5], DHFR/MTX should not require downstream stromal refolding factors. This makes DHFR/MTX an ideal substrate to use in future studies aiming to determine the identity of the import motor(s).

Pore structures in other protein translocons

Access to protein translocon pores is regulated by various gating mechanisms. These include plugging the pore on the cis or trans side of the membrane and/or dynamically opening and closing the transmembrane portion of the pore itself. In the later case, the pore can open/expand via conformational change in the transmembrane domain and/or oligomeric assembly of pore-forming units. The mechanosensitive channel, MscL, is a good example of conformational pore expansion with a dramatic change of 24 Å between the open and closed pores [38]. Examples of all these mechanisms can be found in various protein translocons transporting unfolded or folded substrates.

Bacterial Sec and mitochondrial TOM/TIM translocons require unfolded substrates and have small pores relative to that of TOC/TIC [5]. However, one of the earliest indications of pore expansion during protein translocation came from the ER Sec61 translocon, where the ribosome bound and unbound forms of Sec61 were found to have different channel diameters [39]. Bacterial SecYEG can also undergo pore expansion. A crystal structure of SecY with a linear substrate traversing the pore has a pore diameter of ~8 Å [40]. However, SecYEG is known to transport particles up to 18 Å in diameter [41], indicating there must be significant flexibility in the pore structure. Opening of the SecY lateral gate is likely to contribute to pore expansion [41]. The mitochondrial outer membrane pore-forming Tom40, a 19-stranded β-barrel protein, appears not to expand since the structural and functional pore sizes match [42,43]. A structure is not available for the inner membrane Tim23 pore, but it

does have some flexibility since conformational changes in its pore-forming TMHs have been detected in response to the membrane potential [44]. Opening/closure of the Tim23 pore is also regulated by the soluble domain of Tim50 [45].

Other ubiquitous pathways that translocate folded substrates, peroxisomal import and Tat transport, lack structural details for their pores. Peroxisomes can import large folded proteins and colloidal gold particles 40–90 Å in diameter [46]. These large pores are dynamically generated in the presence of substrate by oligomerization of the pore-forming components, Pex5p and Pex14p [47]. The Tat pathway, found in thylakoid and bacterial membranes, has a mechanism that involves dynamic assembly of the TatA component that somehow contributes to pore formation [48].

Many bacterial secretion system structures have been resolved. The type I secretion system exports unfolded proteins. The type I outer membrane component, TolC, has β-barrel transmembrane domains and helical coiled coil periplasmic domains, which gate the pore by twisting open and closed like an iris [49]. The inner membrane component is part of the ABC transporter family, which operate under an alternative access mechanism with the substrate-binding domain opening to the cis or trans side of the membrane in an ATP-dependent manner [50]. Substrates utilizing the type II secretion system cross the inner membrane via the Sec or Tat pathways and are exported in folded conformations across the outer membrane. The type II pore-forming component, GspD has a β-barrel transmembrane pore, which is gated on both sides of the membrane [51]. These gating domains are pushed aside as the substrate passes through the pore. Type IX secretion system substrates also utilize the Sec pathway to cross the inner membrane. SprA, the type IX outer membrane pore-forming component, exports folded substrates through the largest monomeric membrane β-barrel domain identified to date with 36 transmembrane β-strands. Along with a periplasmic plug protein, the SprA barrel alternatively opens at the cis and trans sides of the membrane, which is accompanied by large conformational changes in the barrel itself [52]. It is interesting to note that all of the bacterial double membrane spanning secretion systems seem to transport unfolded substrates [50]. This is likely because the unique Tat pathway is highly specialized in transporting folded substrates across the energy-transducing inner membrane without leaking ions [53].

Based on the above survey of protein translocon structures, transmembrane pore flexibility is quite common. The functional pore size of the TOC/TIC translocons predicts highly dynamic pores in chloroplasts as well. For example, we expect the pore diameter of the TOC complex to expand up to 10–15 Å between resting and active states (assuming a closed Toc75 resting state). The precise mechanisms will need to await high-resolution structures of these complexes. However, some biochemical approaches, such as those described here, would also further our understanding of the chloroplast protein import pores. The rather unique ability of chloroplasts to translocate folded proteins across a double membrane system via the coupled TOC/TIC translocons warrants further inquiry into the precise structure-functional mechanisms that underlie this feat.

Acknowledgements

This work was supported by Department of Energy Grant DE-SC0017035 to SMT. We thank Laura Klasek for critical reading of the manuscript.

Author contributions

IG and SMT wrote the manuscript.

References

1 Schleiff E, Soll J, Kuchler M, Kuhlbrandt W and Harrer R (2003) Characterization of the translocon of the outer envelope of chloroplasts. *J Cell Biol* **160**, 541–551.

2 Bolter B and Soll J (2016) Once upon a time – chloroplast protein import research from infancy to future challenges. *Mol Plant* **9**, 798–812.

3 Nakai M (2015) The TIC complex uncovered: The alternative view on the molecular mechanism of protein translocation across the inner envelope membrane of chloroplasts. *Biochem Biophys Acta* **1847**, 957–967.

4 Paila YD, Richardson LG and Schnell DJ (2014) New insights into the mechanism of chloroplast protein import and its integration with protein quality control, organelle biogenesis and development. *J Mol Biol* **427**, 1038–1060.

5 Ganesan I, Shi LX, Labs M and Theg SM (2018) Evaluating the functional pore size of chloroplast TOC and TIC protein translocons: import of folded proteins. *Plant Cell* **30**, 2161–2173.

6 Kouranov A and Schnell DJ (1997) Analysis of the interactions of preproteins with the import machinery over the course of protein import into chloroplasts. *J Cell Biol* **139**, 1677–1685.

7 Becker T, Jelic M, Vojta A, Radunz A, Soll J and Schleiff E (2004) Preprotein recognition by the Toc complex. *EMBO J* **23**, 520–530.

8 Hirsch S, Muckel E, Heemeyer F, von Heijne G and Soll J (1994) A receptor component of the chloroplast protein translocation machinery. *Science* **266**, 1989–1992.
9 Kikuchi S, Hirohashi T and Nakai M (2006) Characterization of the preprotein translocon at the outer envelope membrane of chloroplasts by blue native PAGE. *Plant Cell Physiol* **47**, 363–371.
10 Kikuchi S, Bedard J, Hirano M, Hirabayashi Y, Oishi M, Imai M, Takase M, Ide T and Nakai M (2013) Uncovering the protein translocon at the chloroplast inner envelope membrane. *Science* **339**, 571–574.
11 Kuchler M, Decker S, Hormann F, Soll J and Heins L (2002) Protein import into chloroplasts involves redox-regulated proteins. *EMBO J* **21**, 6136–6145.
12 Kessler F and Blobel G (1996) Interaction of the protein import and folding machineries of the chloroplast. *Proc Natl Acad Sci USA* **93**, 7684–7689.
13 Nielsen E, Akita M, Davila-Aponte J and Keegstra K (1997) Stable association of chloroplastic precursors with protein translocation complexes that contain proteins from both envelope membranes and a stromal Hsp100 molecular chaperone. *EMBO J* **16**, 935–946.
14 Su PH and Li HM (2010) Stromal Hsp70 is important for protein translocation into pea and Arabidopsis chloroplasts. *Plant Cell* **22**, 1516–1531.
15 Tsai JY, Chu CC, Yeh YH, Chen LJ, Li HM and Hsiao CD (2013) Structural characterizations of the chloroplast translocon protein Tic110. *Plant J Cell Mol Biol* **75**, 847–857.
16 Noinaj N, Kuszak AJ, Gumbart JC, Lukacik P, Chang H, Easley NC, Lithgow T and Buchanan SK (2013) Structural insight into the biogenesis of beta-barrel membrane proteins. *Nature* **501**, 385–390.
17 Baud C, Guerin J, Petit E, Lesne E, Dupre E, Locht C and Jacob-Dubuisson F (2014) Translocation path of a substrate protein through its Omp85 transporter. *Nat Commun* **5**, 5271.
18 Shiota T, Imai K, Qiu J, Hewitt VL, Tan K, Shen HH, Sakiyama N, Fukasawa Y, Hayat S, Kamiya M *et al.* (2015) Molecular architecture of the active mitochondrial protein gate. *Science* **349**, 1544–1548.
19 Hohr AIC, Lindau C, Wirth C, Qiu J, Stroud DA, Kutik S, Guiard B, Hunte C, Becker T, Pfanner N *et al.* (2018) Membrane protein insertion through a mitochondrial beta-barrel gate. *Science* **359**, eaah6834.
20 Kyte J and Doolittle RF (1982) A simple method for displaying the hydropathic character of a protein. *J Mol Biol* **157**, 105–132.
21 Peterson JH, Hussain S and Bernstein HD (2018) Identification of a novel post-insertion step in the assembly of a bacterial outer membrane protein. *Mol Microbiol* **110**, 143–159.
22 Rial DV, Lombardo VA, Ceccarelli EA and Ottado J (2002) The import of ferredoxin-NADP+ reductase precursor into chloroplasts is modulated by the region between the transit peptide and the mature core of the protein. *Europ J Biochemi/FEBS* **269**, 5431–5439.
23 Richardson LGL, Small EL, Inoue H and Schnell DJ (2018) Molecular topology of the transit peptide during chloroplast protein import. *Plant Cell* **30**, 1789–1806.
24 Wallas TR, Smith MD, Sanchez-Nieto S and Schnell DJ (2003) The roles of toc34 and toc75 in targeting the toc159 preprotein receptor to chloroplasts. *J Biol Chem* **278**, 44289–44297.
25 Iadanza MG, Higgins AJ, Schiffrin B, Calabrese AN, Brockwell DJ, Ashcroft AE, Radford SE and Ranson NA (2016) Lateral opening in the intact beta-barrel assembly machinery captured by cryo-EM. *Nat Commun* **7**, 12865.
26 Noinaj N, Kuszak AJ, Balusek C, Gumbart JC and Buchanan SK (2014) Lateral opening and exit pore formation are required for BamA function. *Structure* **22**, 1055–1062.
27 Shipman-Roston RL, Ruppel NJ, Damoc C, Phinney BS and Inoue K (2010) The significance of protein maturation by plastidic type I signal peptidase 1 for thylakoid development in Arabidopsis chloroplasts. *Plant Physiol* **152**, 1297–1308.
28 Paila YD, Richardson LG, Inoue H, Parks ES, McMahon J, Inoue K and Schnell DJ (2016) Multi-functional roles for the polypeptide transport associated domains of Toc75 in chloroplast protein import. *ELife* **5**, e12631.
29 O'Neil PK, Richardson LGL, Paila YD, Piszczek G, Chakravarthy S, Noinaj N and Schnell D (2017) The POTRA domains of Toc75 exhibit chaperone-like function to facilitate import into chloroplasts. *Proc Natl Acad Sci USA* **114**, E4868–E4876.
30 Alder NN, Jensen RE and Johnson AE (2008) Fluorescence mapping of mitochondrial TIM23 complex reveals a water-facing, substrate-interacting helix surface. *Cell* **134**, 439–450.
31 Flores-Perez U and Jarvis P (2013) Molecular chaperone involvement in chloroplast protein import. *Biochem Biophys Acta* **1833**, 332–340.
32 Inoue H, Li M and Schnell DJ (2013) An essential role for chloroplast heat shock protein 90 (Hsp90C) in protein import into chloroplasts. *Proc Natl Acad Sci USA* **110**, 3173–3178.
33 Kikuchi S, Asakura Y, Imai M, Nakahira Y, Kotani Y, Hashiguchi Y, Nakai Y, Takafuji K, Bedard J, Hirabayashi-Ishioka Y *et al.* (2018) A Ycf2-FtsHi heteromeric AAA-ATPase complex is required for chloroplast protein import. *Plant Cell* **30**, 2677–2703.
34 Tomkiewicz D, Nouwen N and Driessen AJ (2007) Pushing, pulling and trapping–modes of motor protein supported protein translocation. *FEBS Lett* **581**, 2820–2828.

35 Herrmann JM (2018) A force-generating machine in the plant's powerhouse: a pulling AAA-ATPase motor drives protein translocation into chloroplasts. *Plant Cell* **30**, 2646–2647.
36 De Los Rios P, Ben-Zvi A, Slutsky O, Azem A and Goloubinoff P (2006) Hsp70 chaperones accelerate protein translocation and the unfolding of stable protein aggregates by entropic pulling. *Proc Natl Acad Sci USA* **103**, 6166–6171.
37 Sousa R, Liao HS, Cuellar J, Jin S, Valpuesta JM, Jin AJ and Lafer EM (2016) Clathrin-coat disassembly illuminates the mechanisms of Hsp70 force generation. *Nat Struct Mol Biol* **23**, 821–829.
38 Wang Y, Liu Y, Deberg HA, Nomura T, Hoffman MT, Rohde PR, Schulten K, Martinac B and Selvin PR (2014) Single molecule FRET reveals pore size and opening mechanism of a mechano-sensitive ion channel. *ELife* **3**, e01834.
39 Hamman BD, Chen JC, Johnson EE and Johnson AE (1997) The aqueous pore through the translocon has a diameter of 40-60 A during cotranslational protein translocation at the ER membrane. *Cell* **89**, 535–544.
40 Li L, Park E, Ling J, Ingram J, Ploegh H and Rapoport TA (2016) Crystal structure of a substrate-engaged SecY protein-translocation channel. *Nature* **531**, 395–399.
41 Bonardi F, Halza E, Walko M, Du Plessis F, Nouwen N, Feringa BL and Driessen AJ (2011) Probing the SecYEG translocation pore size with preproteins conjugated with sizable rigid spherical molecules. *Proc Natl Acad Sci USA* **108**, 7775–7780.
42 Bausewein T, Mills DJ, Langer JD, Nitschke B, Nussberger S and Kuhlbrandt W (2017) Cryo-EM structure of the TOM core complex from *Neurospora crassa*. *Cell* **170** (693–700), e7.
43 Schwartz MP and Matouschek A (1999) The dimensions of the protein import channels in the outer and inner mitochondrial membranes. *Proc Natl Acad Sci USA* **96**, 13086–13090.
44 Malhotra K, Sathappa M, Landin JS, Johnson AE and Alder NN (2013) Structural changes in the mitochondrial Tim23 channel are coupled to the proton-motive force. *Nat Struct Mol Biol* **20**, 965–972.
45 Meinecke M, Wagner R, Kovermann P, Guiard B, Mick DU, Hutu DP, Voos W, Truscott KN, Chacinska A, Pfanner N *et al*. (2006) Tim50 maintains the permeability barrier of the mitochondrial inner membrane. *Science* **312**, 1523–1526.
46 Walton PA, Hill PE and Subramani S (1995) Import of stably folded proteins into peroxisomes. *Mol Biol Cell* **6**, 675–683.
47 Meinecke M, Cizmowski C, Schliebs W, Kruger V, Beck S, Wagner R and Erdmann R (2010) The peroxisomal importomer constitutes a large and highly dynamic pore. *Nat Cell Biol* **12**, 273–277.
48 Cline K (2015) Mechanistic aspects of folded protein transport by the twin arginine translocase (Tat). *J Biol Chem* **290**, 16530–16538.
49 Pei XY, Hinchliffe P, Symmons MF, Koronakis E, Benz R, Hughes C and Koronakis V (2011) Structures of sequential open states in a symmetrical opening transition of the TolC exit duct. *Proc Natl Acad Sci USA* **108**, 2112–2117.
50 Costa TR, Felisberto-Rodrigues C, Meir A, Prevost MS, Redzej A, Trokter M and Waksman G (2015) Secretion systems in Gram-negative bacteria: structural and mechanistic insights. *Nat Rev Microbiol* **13**, 343–359.
51 Yan Z, Yin M, Xu D, Zhu Y and Li X (2017) Structural insights into the secretin translocation channel in the type II secretion system. *Nat Struct Mol Biol* **24**, 177–183.
52 Lauber F, Deme JC, Lea SM and Berks BC (2018) Type 9 secretion system structures reveal a new protein transport mechanism. *Nature* **564**, 77–82.
53 Teter SA and Theg SM (1998) Energy-transducing thylakoid membranes remain highly impermeable to ions during protein translocation. *Proc Natl Acad Sci USA* **95**, 1590–1594.
54 Kelley LA, Mezulis S, Yates CM, Wass MN and Sternberg MJ (2015) The Phyre2 web portal for protein modeling, prediction and analysis. *Nat Protoc* **10**, 845–858.
55 Lai JY, Poon YS, Kaiser JT and Rees DC (2013) Open and shut: crystal structures of the dodecylmaltoside solubilized mechanosensitive channel of small conductance from *Escherichia coli* and *Helicobacter pylori* at 4.4 A and 4.1 A resolutions. *Protein Sci* **22**, 502–509.
56 Chang G, Spencer RH, Lee AT, Barclay MT and Rees DC (1998) Structure of the MscL homolog from *Mycobacterium tuberculosis*: a gated mechanosensitive ion channel. *Science* **282**, 2220–2226.
57 Dong C, Beis K, Nesper J, Brunkan-Lamontagne AL, Clarke BR, Whitfield C and Naismith JH (2006) Wza the translocon for *E. coli* capsular polysaccharides defines a new class of membrane protein. *Nature* **444**, 226–229.
58 Mueller M, Grauschopf U, Maier T, Glockshuber R and Ban N (2009) The structure of a cytolytic alpha-helical toxin pore reveals its assembly mechanism. *Nature* **459**, 726–730.
59 Rodriguez F, Rouse SL, Tait CE, Harmer J, De Riso A, Timmel CR, Sansom MS, Berks BC and Schnell JR (2013) Structural model for the protein-translocating element of the twin-arginine transport system. *Proc Natl Acad Sci USA* **110**, E1092–E1101.